

# Geometric Potential Force for the Deformable Model

Si Yong Yeo<sup>1</sup>  
465186@swansea.ac.uk

Xianghua Xie<sup>2</sup>  
x.xie@swansea.ac.uk

Igor Sazonov<sup>1</sup>  
i.sazonov@swansea.ac.uk

Perumal Nithiarasu<sup>1</sup>  
p.nithiarasu@swansea.ac.uk

<sup>1</sup> School of Engineering, Swansea University Swansea SA2 8PP, UK

<sup>2</sup> Department of Computer Science, Swansea University Swansea SA2 8PP, UK

---

## Abstract

We propose a new external force field for deformable models which can be conveniently generalized to high dimensions. The external force field is based on hypothesized interactions between the relative geometries of the deformable model and image gradients. The evolution of the deformable model is solved using the level set method. The dynamic interaction forces between the geometries can greatly improve the deformable model performance in acquiring complex geometries and highly concave boundaries, and in dealing with weak image edges. The new deformable model can handle arbitrary cross-boundary initializations. Here, we show that the proposed method achieve significant improvements when compared against existing state-of-the-art techniques.

## 1 Introduction

Deformable models are curves and surfaces that deform under the influence of internal and external forces to delineate an object boundary in an image. These deformable model based approaches have been widely used for shape extraction due to their natural handling of shape variation [1, 2, 3, 4]. Explicit deformable models [5, 6] represent contours and surfaces in their parametric form during deformation. This allows explicit models to track the points on the curves and surfaces across time, and is well suited for real-time applications due to the fast computation time. However, explicit models generally have difficulties in dealing with topological changes. Implicit deformable models based on the level set method [7, 8, 9] are introduced to address some of the limitations. In this approach, the evolution of curves and surfaces are represented implicitly as a level set of a higher-dimensional scalar function and the deformation of the model is based on geometric measures such as the unit normal and curvature. Thus the evolution is independent of the parameterization, and topological changes such as splitting and merging can be handled automatically.

The design of deformable models often varies in the representation of the object boundary and external force field used. There have been numerous work involved in the design and

improvement of the underlying techniques. These usually take the form of image gradient based approaches *e.g.* [1, 2, 3, 4, 5], region based approaches *e.g.* [6, 7] and hybrid approaches *e.g.* [8, 9]. It is also a great challenge for deformable models to achieve initialization invariancy and robust convergence. This is especially true when the deformable model has to deal with complex geometries and concave shapes.

In this paper, a novel external force field that is based on the relative position and orientation of the deformable model and object boundaries is proposed. This force field is called the *geometric potential force (GPF) field* as it is based on the hypothesized interactions between the relative geometries of the deforming surface and the object boundaries (characterized by image gradients). The evolution of the deformable model is solved using the level set method. The proposed external force field can attract the deformable model to object boundaries with arbitrary initialization, and allows the deformable model to reach highly concave regions which are generally difficult for other methods. The proposed method can be considered as a generalization of the 2D MAC model [10], whose analogy based on magnetostatics can not be directly applied to 3D or higher dimensional space.

The rest of the paper is organized as follows. In Section 2, we review several image gradient based methods, particularly some physics-inspired approaches, which are closely related to our method. The proposed method is then described in Section 3. The results and comparative studies appear in Section 4. Section 5 concludes the paper.

## 2 Background

In image gradient based deformable models, it is assumed that object boundaries collocate with image intensity discontinuities, which is widely used in computer vision applications. Region based techniques, on the other hand, assume that each object has its own distinctive and continuous regional features, which is not always true for real world data due to intensity inhomogeneity and multi-modal nature. Conventional image gradient based methods, *e.g.* geodesic active contour model [11] and its subsequent incremental improvements such as [12], have difficulties in dealing with boundary concavities, weak edges, image noise and difficult initializations as they are generally prone to local minima that often appear in real images. Numerous research works have been performed to improve the gradient based approaches.

The Gradient Vector Flow (GVF) and its generalized version GGVF [13, 14] have been shown significant improvements over those conventional external force field such as [11] and have been widely used in deformable models, *e.g.* [15]. It uses a vector diffusion equation that diffuses the gradient of an edge map in regions distant from the object boundary. The GGVF has been shown to improve the capture range and boundary concavities tracking ability of deformable models. Although the vector field is bidirectional in nature, it can only prevent the deformable contour or surface from leaking through small boundary gaps or weak edges to some extent. It also has convergence issues caused by saddle or stationary points in its force field *i.e.* when the contour is tangent to the force vector [1, 16, 17]. More recent attempts, such as [18, 19, 20] showed promising but limited success.

Recently, there have been several research works on physics-based deformable models such as [21, 22, 23]. In [21], a charged-particle model (CPM) based on electrostatics was applied to attract particles toward object boundaries. The authors in [21] hypothesized a set  $\Omega$  of freely moving particles with the same positive charge  $q$  in an external electrostatic field, generated by fixed negative charges  $e_x$  proportional to the image gradient  $|\nabla u(\mathbf{x})|$  at point  $\mathbf{x}$ . The positively charged particles are attracted towards the fixed negative charges under the

influence of the external particle-mesh Coulomb force  $\mathbf{F}_a$  and repelled by each other by the particle-particle Coulomb force  $\mathbf{F}_r$ . These forces acting on a moving particle at position  $\mathbf{x}$  can be computed as the sums

$$\mathbf{F}_a(\mathbf{x}) = \frac{q}{4\pi\epsilon} \sum_{\mathbf{x}' \neq \mathbf{x}} e_{\mathbf{x}'} \frac{\hat{\mathbf{f}}_{\mathbf{x}\mathbf{x}'}}{r_{\mathbf{x}\mathbf{x}'}}^2, \quad \mathbf{F}_r(\mathbf{x}) = \frac{q^2}{4\pi\epsilon} \sum_{\substack{\mathbf{x}' \in \Omega \\ \mathbf{x}' \neq \mathbf{x}}} \frac{\hat{\mathbf{f}}_{\mathbf{x}\mathbf{x}'}}{r_{\mathbf{x}\mathbf{x}'}}^2 \quad (1)$$

where  $\epsilon$  is the permittivity, and  $\hat{\mathbf{f}}_{\mathbf{x}\mathbf{x}'}$  is the unit vector pointed from  $\mathbf{x}$  to  $\mathbf{x}'$ ,  $r_{\mathbf{x}\mathbf{x}'} = |\mathbf{x} - \mathbf{x}'|$  is the distance between these two points. The total force acting on a particle is given by  $\mathbf{F} = w_a \mathbf{F}_a + w_r \mathbf{F}_r + \beta \mathbf{F}_d$  where  $w_a$ ,  $w_r$  and  $\beta$  are weighting parameters for the attraction force  $\mathbf{F}_a$ , repulsion force  $\mathbf{F}_r$  and damping force  $\mathbf{F}_d$  respectively. When the particles attain a stable equilibrium state due to the viscous effect of  $\mathbf{F}_d$ , contour reconstruction is required to obtain the object boundary representation. Although this approach can resolve the above-mentioned convergence issues, the fact that particles on weak edges may be attracted to nearby strong edges often causes broken contours to be formed. In addition, the method requires frequent particle insertion and deletion, which is computationally expensive. This makes it impractical in 3D. In [14], the authors incorporated the particle model [5] into a contour model and showed subsequent improvements on the CPM. In their approach, a positively charged active contour moving in an hypothesized electrostatic field with field strength proportional to image gradient magnitudes, is attracted to image edges based on a boundary attraction force based on the particle-mesh force described in (1). A boundary competition force is then used to repel nearby free contours from moving towards the already occupied image boundary. The repulsion force was designed in a way such that contours that have reached object boundaries will exert repulsion forces upon other contours while being minimally affected by other contours. However, the dominant external force field is static and its dynamic behavior due to repulsion force can be difficult to predict.

Li and Acton in [8] used a vector field convolution of the image edge map as an external force to attract the active contour towards image boundaries. The vector field kernel  $\mathbf{k}(\mathbf{x})$  consists of radial symmetric vectors pointing towards the center of the kernel, and is given as  $\mathbf{k}(\mathbf{x}) = m(\mathbf{x}) \hat{\mathbf{x}}$ , where  $m(\mathbf{x})$  is the magnitude,  $\hat{\mathbf{x}} = -\mathbf{x}/r$  is the unit vector pointing to the kernel origin,  $r = |\mathbf{x}|$  is the distance from the kernel origin. The magnitude  $m(\mathbf{x})$  of the vector field kernel should be a decreasing positive function of distance from the origin, and can be given as  $m(\mathbf{x}) = (r + \epsilon)^{-\gamma}$  which is inspired by the gravitational law, or  $m(\mathbf{x}) = e^{-r^2/\zeta^2}$  which is a Gaussian shape function, where  $\gamma$  and  $\zeta$  are positive parameters to control the decrease, and  $\epsilon$  is a small positive constant to prevent division by zero at the origin. The vector field convolution can then be written as

$$\mathbf{F}(\mathbf{x}) = f(\mathbf{x}) * \mathbf{k}(\mathbf{x}) := \sum_{\mathbf{h} \in Q_R} f(\mathbf{x} - \mathbf{h}) \mathbf{k}(\mathbf{h}) \quad (2)$$

where  $f(\mathbf{x}) = \nabla u(\mathbf{x})$  is the image edge map and  $Q_R$  is the cube of the edge length  $2R$  centered at the kernel origin. The authors showed better initialization and noise insensitivity in their method. However the generated field is static and cannot handle the convergence issues discussed above.

In [13], Xie and Mirmehdi introduced an external force field is based on the hypothesized magnetic force between the active contour and object boundaries. Given two elements  $dl_1$  and  $dl_2$  of contours with currents  $I_1$  and  $I_2$ , and unit tangent vectors  $\hat{\mathbf{t}}_1$  and  $\hat{\mathbf{t}}_2$ , respectively,

the magnetic flux density  $d\mathbf{B}$  created by the element  $dl_2$  and the corresponding force  $d\mathbf{F}$  acting on  $dl_1$  due to  $dl_2$  are

$$d\mathbf{B} = \frac{\mu_0}{4\pi} \frac{I_2 dl_2}{r_{21}^2} (\hat{\mathbf{t}}_2 \times \hat{\mathbf{r}}_{21}), \quad d\mathbf{F} = I_1 dl_1 (\hat{\mathbf{t}}_1 \times d\mathbf{B}) \quad (3)$$

where  $r_{21}$  is the distance between elements  $dl_2$  and  $dl_1$ ,  $\hat{\mathbf{r}}_{21}$  is the unit vector pointing from  $dl_2$  to  $dl_1$ . Note the image is considered as a 2D plane in a 3D space whose origin coincides with the origin of the image coordinates, and the third dimension of this 3D space is considered perpendicular to the image plane. This formulation has been applied directly in the magnetostatic active contour (MAC) [18] to compute the magnetic field and force required to draw the active contour towards object boundaries in 2D images. This image gradient based method showed significant improvements on convergence issues, e.g. reaching deep concavities, and in handling weak edges and broken boundaries. While applying the analogy directly to deformable modeling it requires estimation of tangent vectors for the deformable contours, which is convenient in 2D case, however, not possible in 3D.

Kimmel in [9] proposed a hybrid method that use an alignment measure together with the geodesic active contour and minimal variance criterion suggested by [9]. Given a contour  $C$  of length  $L$ , and in a parametric form  $C(s) = \{\mathbf{x}(s)\}$  where  $s$  is an arclength parameter, the alignment measure used in [9] is given as

$$E(C) = \int_0^L |\nabla u[\mathbf{x}(s)] \cdot \hat{\mathbf{n}}(s)| ds \quad (4)$$

where  $\hat{\mathbf{n}}(s)$  is the unit normal to contour  $C$  at  $s$ ,  $\nabla u(\mathbf{x})$  is the image gradient at  $\mathbf{x}$ . The alignment measure is used to optimize the orientation of the curve with respect to the image gradients. This measure, together with the gradient-based geodesic measure and the region-based minimal variance criterion is then used to push or pull the contour towards the image boundary. This hybrid approach, however, requires careful tuning of the different parameters associated with the various measures in order to efficiently bridge the image gradient and regional information. In addition, only local edge information are used in the alignment measure, while edge information of pixels located away from the contour are not considered in this technique.

### 3 Proposed Method

Our approach is to define a novel external force field that is based on hypothesized geometrically induced interactions between the relative geometries of the deformable model and the object boundaries (characterized by image gradients). In other words, the magnitude and direction of the interaction forces are based on the relative position and orientation between the geometries of the deformable model and image object boundaries, and hence, it is called the *geometric potential force (GPF)* field. The bidirectionality of the new external force field can facilitate arbitrary cross-boundary initialization, which is a very useful feature to have, especially in the segmentation of complex geometries. It also improves the performance of the deformable model in handling weak edges. In addition, the proposed external force field is dynamic in nature as it changes according to the relative position and orientation between the evolving deformable model and object boundary.

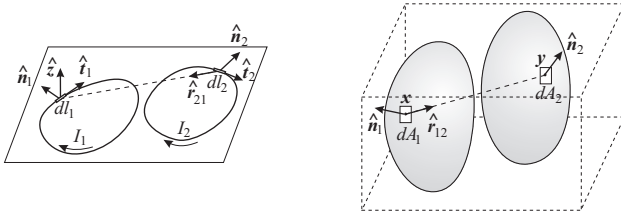


Figure 1: Relative position and orientation between geometries of 2D contours (left) and 3D surfaces (right).

### 3.1 Geometric potential force

Consider two elements  $dl_1$  and  $dl_2$  on two contours, with unit normals  $\hat{\mathbf{n}}_1$  and  $\hat{\mathbf{n}}_2$  respectively (refer to Fig. 1). The hypothesized interaction force  $d\mathbf{F}$  acting on  $dl_1$  due to  $dl_2$  is given as

$$d\mathbf{F} = dl_1 \hat{\mathbf{n}}_1 dG, \quad dG = \frac{dl_2}{r_{12}^k} (\hat{\mathbf{r}}_{12} \cdot \hat{\mathbf{n}}_2) \quad (5)$$

where  $dG$  is considered as the geometrically induced potential created by element  $dl_1$ . Here,  $\hat{\mathbf{n}}_2$  is the unit normal to the contour at element  $dl_2$ ,  $r_{12}$  is the distance between  $dl_1$  and  $dl_2$ , and  $\hat{\mathbf{r}}_{12}$  is the unit vector pointing from  $dl_1$  to  $dl_2$ ;  $k$  is a positive constant that affects the magnitude of the interaction force based on the distance between  $dl_1$  and  $dl_2$ , and is set to the same as the dimension of the image data. The geometric potential  $dG$  can be seen as an induced scalar field, in which the strength of  $dG$  depends on the relative position of the two elements  $dl_1$  and  $dl_2$ . The magnitude and direction of the geometrically induced vector force  $d\mathbf{F}$  is therefore handled intrinsically by the relative position and orientation between the geometries of the deformable model and object boundary.

Here we also show that (5) can be re-written in a different form using tangent vectors  $\hat{\mathbf{t}}_1$  and  $\hat{\mathbf{t}}_2$  at  $dl_1$  and  $dl_2$  respectively. Let vector  $\hat{\mathbf{z}} = (0, 0, 1)$  be the normal to the plane where the active contour and object boundary are lying on. The unit normals on the length elements can now be represented as  $\hat{\mathbf{n}}_1 = \hat{\mathbf{z}} \times \hat{\mathbf{t}}_1$  and  $\hat{\mathbf{n}}_2 = \hat{\mathbf{z}} \times \hat{\mathbf{t}}_2$ , and the induced force  $d\mathbf{F}$  and the vector potential  $d\mathbf{G} = (0, 0, dG)$  can now be written as

$$d\mathbf{F} = dl_1 (\hat{\mathbf{t}}_1 \times d\mathbf{G}), \quad d\mathbf{G} = \frac{|\hat{\mathbf{z}} \times \hat{\mathbf{t}}_2| dl_2}{r_{12}^k} (\hat{\mathbf{t}}_2 \times \hat{\mathbf{r}}_{12}) \quad (6)$$

We note that the formulation in (6) is analogous to the force field adapted from the theory of magnetostatics used on 2D images in [18] (see (3)), however, the new external force field has a different physical meaning compared to the traditional magnetic force field. Note that the magnetic force field used in [18] requires the estimation of the hypothesized current directions represented by the tangent vectors  $\hat{\mathbf{t}}_1$  and  $\hat{\mathbf{t}}_2$ . To deal with this requirement, the authors in [18] compute the direction of the imposed currents for the active contour and object boundary by rotating the respective gradient vectors in a clockwise or counter-clockwise manner such that a current loop is formed on both the active contour and object boundary. It is however difficult to extend MAC to handle 3D images directly as it is not apparent how the hypothesized current direction is to be estimated and set on a 3D object.

As shown in (5), the computation of the new force field only requires unit normal vectors and relative position of the two elements, which is easy to acquire. Thus, this new force field

can be easily extended to higher dimensions, and a generalized 3D version of the GPF acting between two area elements  $dA_1$  and  $dA_2$  (see Fig. 1) can be readily given as

$$d\mathbf{F} = dA_1 \hat{\mathbf{n}}_1 dG, \quad dG = \frac{dA_2}{r_{12}^k} (\hat{\mathbf{r}}_{12} \cdot \hat{\mathbf{n}}_2) \quad (7)$$

where  $dG$  the corresponding 3D potential field, and  $\hat{\mathbf{n}}_1$  and  $\hat{\mathbf{n}}_2$  are unit surface normals.

Note the alignment term in [7] as shown in (4) also uses the conformity between image gradient vectors and deformable contour/surface normals. However, this alignment test in [7] is carried out locally and relies on the geodesic and minimal variance terms to further propagate the deformable model. The proposed GPF model utilizes edge-pixel interactions across the entire image domain, which provides a more global view of object boundary representation. Thus, we do not need any additional terms to regulate the deformable model which minimizes parameter tuning and uncertainty in contour/surface evolution.

The physics-based deformable models described in [5, 8, 21] all use a kernel based function to compute the external force field. These kernels all consist of a decreasing function of distance  $r$  from the origin, in the form of  $\mathbf{r}/r^n$ , where  $\mathbf{r}$  is the vector pointing to or from the kernel origin, and  $n$  is a positive constant. In [8], the external force is calculated by convolving a vector field with the edge map. One of the vector field kernel described, resembles the gravitational law in physics, such that edge pixels in the edge map were considered as objects with mass proportional to the edge strength, which is fundamentally very similar to the electrostatic force used in [5, 21]. Another vector field kernel used comes in the form of a Gaussian shape function where the influence of the image edge strength increases as the standard deviation increases. These kernels however only takes into consideration of regional pixels, and the resulting force field is static. The authors in [21] incorporated the CPM [5] into their deformable models. Similar to [8], they used a kernel function that decides the influence of the edge pixels on the magnitude of the force based on their distance from the kernel origin, but in a more global sense. It however requires an image dependent boundary competition force to repel nearby free contours from being attracted to the already occupied image edge. Also, the balance between the attraction force and the boundary competition force used in this technique largely affects the convergence of contours and sometimes requires careful tuning. The proposed GPF model not only considers the global information of the image, but also the relative orientation of the deformable model and object boundary, which greatly improve the deformable model performance in handling complex shapes.

### 3.2 GPF deformable model

Let the 3D image be described by function  $u(\mathbf{x})$  where  $\mathbf{x}$  is a pixel or voxel location in the image domain, and  $\nabla u$  be its gradient. Let  $dA_1$  belongs to the deformable surface whereas  $dA_2$  belongs to the object boundary. To compute the force acting on  $dA_1$  from  $dA_2$ , we substitute  $\hat{\mathbf{n}}_2 = \nabla u / |\nabla u|$  into (7) and treat  $\mathbf{n}_2$  as a normal to the object boundary. Then we compute the total geometric potential field strength  $G(\mathbf{x})$  at every voxel. Note that only voxels on the object boundary will contribute to the geometric interaction field. Let  $S$  denote the set containing all the edge voxels, and  $\mathbf{y}$  denote a boundary voxel, the total geometric interaction at  $\mathbf{x}$  can then be computed as:

$$G(\mathbf{x}) = \sum_{\mathbf{y} \in S, \mathbf{y} \neq \mathbf{x}} \frac{\hat{\mathbf{r}}_{12}}{r_{12}^k} \cdot \hat{\mathbf{n}}_2(\mathbf{y}) |\nabla u(\mathbf{y})| dA_2 \quad (8)$$

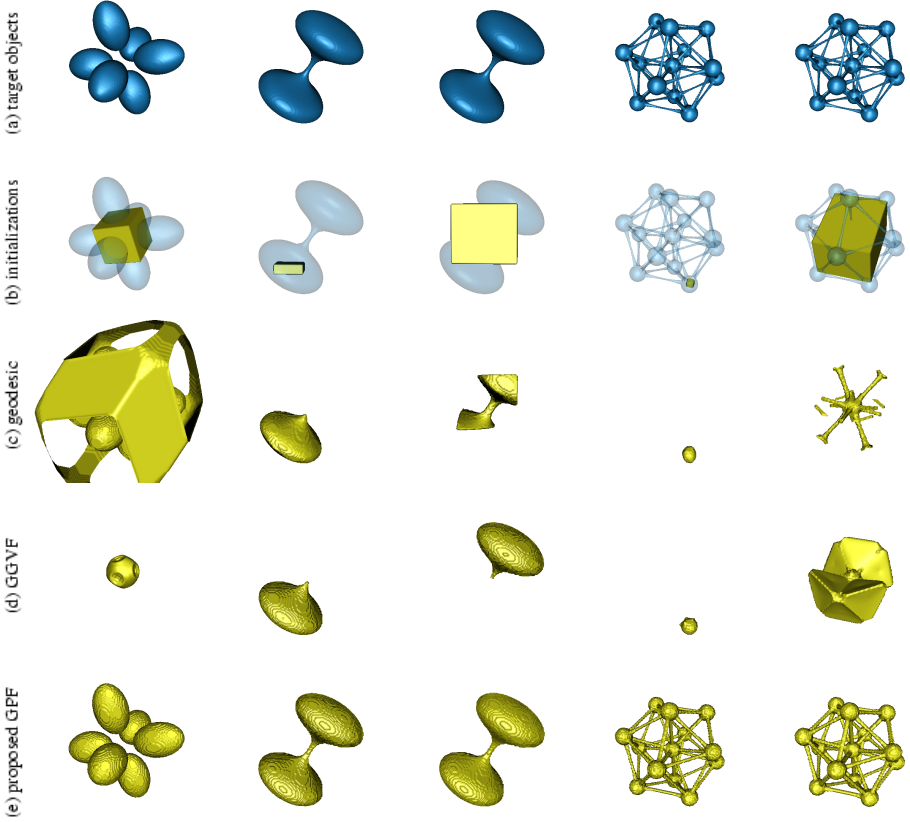


Figure 2: Shape recovery from synthetic images: (a) isosurfaces of various shapes to be recovered from synthetic images ( $128 \times 128 \times 128$ ), (b) initial deformable models (yellow) with input shapes (blue, semi-transparent), (c) recovered shape using geodesic, (d) GGVF, (e) proposed GPF

where  $\hat{\mathbf{r}}_{12}$  is the unit vector from  $\mathbf{x}$  to  $\mathbf{y}$ , and  $r_{12}$  is the distance between them. Computation of (8) is based on the 3D FFT. The force acting due to the geometrically induced potential field on the deformable surface  $\mathcal{L}$  at the position  $\mathbf{x} \in \mathcal{L}$  can then be given as:

$$\mathbf{F}(\mathbf{x}) = dA_1 \hat{\mathbf{n}}(\mathbf{x}) G(\mathbf{x}) \quad (9)$$

Given the force field  $\mathbf{F}(\mathbf{x})$  derived from the hypothesized interactions based on the relative geometries of the deformable model and object boundary, the evolution of the deformable model  $C(\mathbf{x}, t)$  under this force field can be given as:  $C_t = (\mathbf{F} \cdot \hat{\mathbf{n}}) \hat{\mathbf{n}}$ . Since contour or surface smoothing is usually desirable, the mean curvature flow is added and the complete geometric potential deformable model evolution can be formulated as:

$$C_t = \alpha g(\mathbf{x}) \kappa \hat{\mathbf{n}} + (1 - \alpha)(\mathbf{F} \cdot \hat{\mathbf{n}}) \hat{\mathbf{n}} \quad (10)$$

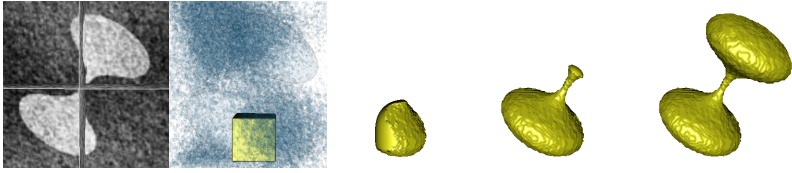


Figure 3: Shape recovery from noisy image.



Figure 4: Shape recovery from weak edges.

where  $g = \frac{1}{1+|\nabla u|}$  is the stopping function. Its level set representation can then be given as:

$$\Phi_t = \alpha g \kappa |\nabla \Phi| - (1 - \alpha)(\mathbf{F} \cdot \nabla \Phi) \quad (11)$$

## 4 Results and Discussion

In this section, we present experimental results on both synthetic and real image data. Fig. 2 provides a comparative analysis on various shape geometries and topologies. These shapes are generated in the form of synthetic binary images, and they include the six-ellipsoids problem, objects with deep concavities, and objects with complex geometry and topology. Applying CPM [5] to 3D data is computationally impractical. Moreover, it requires reconstructing surfaces from unstructured 3D points. The vector kernel convolution force field [8] is static which is the same as GGVF. Note the MAC model [18] can not be directly applied to 3D data. Thus, we provide the comparative results of the proposed method against geodesic and GGVF deformable models.

The first column in Fig. 2 shows the shape extraction results for the six-ellipsoids problem. Given an arbitrary initialization across all the ellipsoids, only GPF could accurately recover the shapes. The geodesic model cannot handle the cross-boundary initialization as the constant pressure term can only monotonically shrink or expand the contour. The saddle and stationary points in this example prevented GGVF from extracting the ellipsoids.

Next, we compare the ability of the deformable models to deal with highly concave boundaries. As shown in the second and third columns in Fig. 2, the shape object to be recovered consists of two flattened ellipsoids connected by a narrowing tube with a constriction in the middle. With the deformable models initialized inside one of the ellipsoid, only GPF could propagate through the narrowing tube to accurately extract the shape. Also, with a more arbitrary cross-boundary initialization, GPF was the only successful model to extract the exact shape. The other two methods could neither handle the arbitrary initialization nor propagate through deep concavities. Note the bottleneck between the two ellipsoids is extremely narrow, which makes it particularly difficult for geodesic model to propagate through without stepping through the object boundary due to large expansion force.

The fourth and fifth columns in Fig. 2 compares the shape extraction results on a complex geometry with different initialization configurations. It is shown that GPF is the only model to successfully extract the geometry. The above examples demonstrate the superior performance of the GPF deformable model in resolving deep concavities and handling complex geometries and topologies. This is mainly due to the dynamic nature of the vector force field. In addition, we show that the bidirectionality of the force field gives GPF the flexibility to deal with arbitrary cross-initializations.

Fig. 3 shows the performance of the proposed method on noisy images. It accurately extracted the shape from an image with significant amount of noise. Note the noise made the marching cube based algorithm impossible to render the target object (cf. Fig. 2). In Fig. 4, we provide an example of recovering a star-like 3D shape from a substantially blurred image data. Note no dedicated initialization was required for the proposed method.

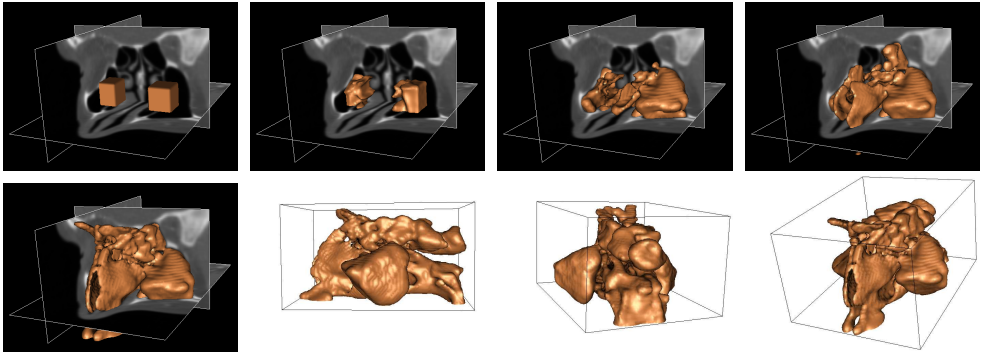


Figure 5: Segmentation process of human nasal cavity using the GPF deformable model.

Figs. 5 and 6 shows the GPF deformable model in the segmentation of the human nasal cavity with very complex geometries and human aorta from medical images acquired from computed tomography (CT) imaging. The initial surfaces are placed across different structures in both the image dataset to demonstrate the capability of the new deformable model to deal with arbitrary cross-initializations. It is shown that the GPF deformable model can efficiently segment thin and complex structures, and can handle inhomogeneity in image intensities and weak edges, which are common in medical images.

## 5 Conclusion

We proposed a novel external force field for the deformable model that is based on hypothesized geometrically induced interactions between the deformable contour or surface and the object boundary. The proposed GPF deformable model can handle arbitrary cross-boundary initializations, and resolve saddle and stationary points issues due to its unique bidirectionality. In addition, the new vector force field is dynamic in nature, and as such, can attract the deformable model into highly concave regions, and propagate through long thin structures. The comparative study on various geometries and topologies showed significant improvements in convergence capability and initialization invariance on existing state-of-the-art methods. The proposed image gradient based deformable model provides an effective alternative approach to region based methods for segmenting complex structures in 3D image data.

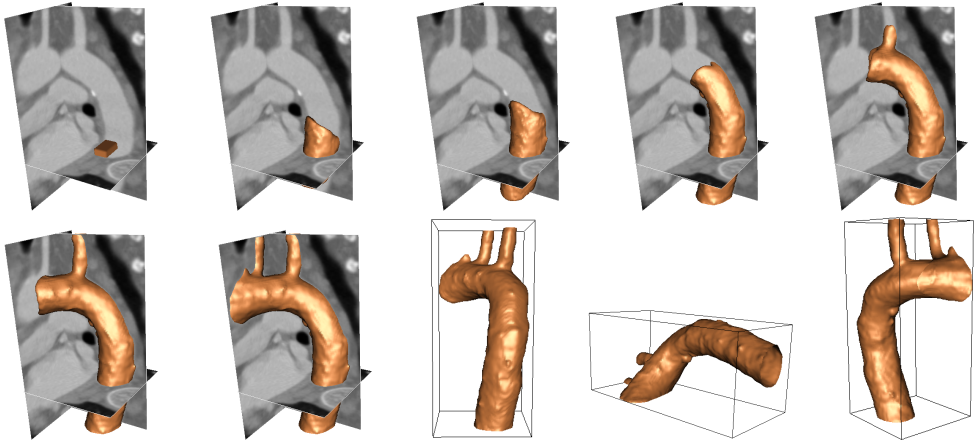


Figure 6: Segmentation of human aorta using the GPF deformable model.

## References

- [1] V. Caselles, F. Catte, T. Coll, and F. Dibos. A geometric model for active contours. *Numerische Mathematik*, 66:1–31, 1993.
- [2] T. Chan and L. Vese. Active contours without edges. *IEEE Transactions on Image Processing*, 10(2):266–277, 2001.
- [3] D. Cremers, M. Rousson, and R. Deriche. A review of statistical approaches to level set segmentation: Integrating color, texture, motion and shape. *International Journal of Computer Vision*, 72(2):195–215, 2007.
- [4] D. Gil and P. Radeva. Curvature vector flow to assure convergent deformable models for shape modelling. In *Energy Minimization Methods in Computer Vision and Pattern Recognition*, pages 357–372, 2003.
- [5] A. Jalba, M. Wilkinson, and J. Roerdink. Cpm: A deformable model for shape recovery and segmentation based on charged particles. *pami*, 26(10):1320–1335, 2004.
- [6] M. Kass, A. Witkin, and T. Terzopoulos. Snakes: Active contour models. *International Journal of Computer Vision*, 1(4):321–331, 1987.
- [7] R. Kimmel. Fast edge integration. In *Geometric Level Set Methods in Imaging, Vision, and Graphics*, pages 59–77, 2003.
- [8] B. Li and S. Acton. Active contour external force using vector field convolution for image segmentation. *IEEE Transactions on Image Processing*, 16(8):2096–2106, 2007.
- [9] C. Li, J. Liu, and M. Fox. Segmentation of edge preserving gradient vector flow: an approach toward automatically initializing and splitting of snakes. In *IEEE Conference on Computer Vision Pattern Recognition*, pages 162–167, 2005.
- [10] R. Malladi, J. A. Sethian, and B. C. Vemuri. Shape modelling with front propagation: A level set approach. *IEEE Transactions on Pattern Analysis and Machine Intelligence*, 17(2):158–175, 1995.

- [11] T. McInerney and D. Terzopoulos. Deformable models in medical image analysis: A survey. *Medical Image Analysis*, 1(2):91–108, 1996.
- [12] N. Paragios, O. Mellina-Gottardo, and V. Ramesh. Gradient vector flow geometric active contours. *IEEE Transactions on Pattern Analysis and Machine Intelligence*, 26(3):402–407, 2004.
- [13] N. Ray and S. Acton. Motion gradient vector flow: An external force for tracking rolling leukocytes with shape and size constrained active contours. *IEEE Transactions on Medical Imaging*, 23(12):1466–1478, 2004.
- [14] J. A. Sethian. *Level Set Methods and Fast Marching Methods: Evolving Interfaces in Computational Geometry, Fluid Mechanics, Computer Vision, and Material Science*. Cambridge University Press, Cambridge, UK, 1999.
- [15] K. Siddiqi, Y. Lauzière, A. Tannenbaum, and S. Zucker. Area and length minimizing flows for shape segmentation. *IEEE Transactions on Image Processing*, 7(3):433–443, 1998.
- [16] R. Whitaker. Modeling deformable surfaces with level sets. *IEEE Computer Graphics and Applications*, 24(5):6–9, 2004.
- [17] X. Xie and M. Mirmehdi. RAGS: Region-aided geometric snake. *IEEE Transactions on Image Processing*, 13(5):640–652, 2004.
- [18] X. Xie and M. Mirmehdi. MAC: Magnetostatic active contour model. *IEEE Transactions on Pattern Analysis and Machine Intelligence*, 30(4):632–647, 2008.
- [19] C. Xu and J. L. Prince. Snakes, shapes, and gradient vector flow. *IEEE Transactions on Image Processing*, 7(3):359–369, 1998.
- [20] C. Xu and J. L. Prince. Generalized gradient vector flow external forces for active contours. *Signal Processing*, 71(2):131–139, 1998.
- [21] R. Yang, M. Mirmehdi, and X. Xie. A charged active contour based on electrostatics. In *Advanced Concepts for Intelligent Vision Systems*, pages 173–184, 2006.